LITERATURE CITED

1. Yu. I. Meshcheryakov, V. A. Morozov, and Yu. V. Suden'kov, "Experimental methods of examining highly nonequilibrium processes in solids on exposure to pulsed electron beams and high-speed collision," in: Physical Mechanics [in Russian], Issue 2, Izd. LGU, Leningrad (1978).
2. L. M. Barker, Behavior of Dense Media under High Dynamic Pressure, Gordon and Breach, New York (1968).
3. R. A. Graham, F. W. Neilson, and W. B. Benedic, "Piezoelectric current from shock loaded quartz: a submicrosecond stress gauge," J. Appl. Phys., 36, No. 5 (1965).
4. L. M. Barker, "α-phase Hugoniot in iron," J. Appl. Phys., 46, No. 6 (1975).
5. J. R. Asay and L. M. Barker, "Interferometric measurements of shock-induced internal particle velocity and spatial variation of particle velocity," J. Appl. Phys., 45, No. 6 (1974).
6. J. N. Johnson and L. M. Barker, "Dislocation dynamics and steady plastic wave profile in 6061-T6 aluminum," J. Appl. Phys., 40, No. 11 (1969).

PORE GROWTH IN SLIP BANDS IN LOCALIZED PLASTIC STRAIN

V. M. Segal

UDC 539.375.5

Pore behavior in a plastically deformed material is of considerable interest in relation to viscous failure [1]. Solutions have been obtained [2, 3] for isolated pores acted on by homogeneous stress and velocity fields applied at infinity; a continuum description has also been given [4, 5] of a plastically dilating material containing a pore ensemble. In all cases it is assumed that the flow in the region of the pores is stable, while the initial spherical or cylindrical shape remains close to equilibrium.

On the other hand, a feature common to all plastic bodies is that the flow is unstable which leads to regions of highly localized strain [6]. Such regions are observed at the microscopic and macroscopic levels as thin shear bands, within which the strain intensity is higher than that in parts outside by several orders of magnitude. The geometrical or material instability [6] determines whether the shear bands occupy fixed positions within the flow regions (lines of velocity discontinuity for the rigid-plastic body) or certain volumes in the deformed material (grain boundaries and other structural imperfections). Also, they can be observed not only directly after the start of plastic flow but also in the final stages preceding failure.

Flow localization and the subsequent strain in slip bands are closely related to pore nucleation and growth. It has been suggested [7] that the localization is due to softening arising from the increase in porosity. An alternative view [6] relates the localization to detailed features of the constructive equations. However, no matter what the reasons, localization produces a considerable reduction in the plasticity because the strain is concentrated in small volumes and a specific mechanism occurs for pore growth in the shear bands. The latter is accompanied by the formation of pore layers, in which viscous cracks grow and the material fails. As the thicknesses of the shear bands hardly alter during this process, it is clear that the pore shape becomes nonequilibrium at the localization stage, while the change in pore size occurs mainly in the shear planes. This conclusion is confirmed by analogous stability-loss phenomena for pores in pure shear in elastic and viscous materials [8]. Neglect of this feature should result in one substantially overestimating the plasticity parameters, as is observed in the analysis of viscous failure in shear bands [9, 10] based on an isotropic pore growth mechanism [5].

Here we present a simple model for pore behavior during plastic-strain localization, which involves pronounced anisotropy in the growth rates in the shear plane and in the normal direction. The results are applied in examining the formation of viscous cracks along velocity-discontinuity lines for a rigid-plastic material in pressure-working of metals.

Minsk. Translated from Zhurnal Prikladnoi Mekhaniki i Tekhnicheskoi Fiziki, No. 1, pp. 127-134, January-February, 1984. Original article submitted November 10, 1982.

0021-8944/84/2501-0114$08.50

1. Consider a material containing a rigid-plastic matrix with uniformly distributed pores. The material in the initial state is assumed to be macroscopically homogeneous and isotropic; the structural parameters are determined by the average pore dimensions $2a$ and the distances between them 2A. The porosity

$$\theta = (a/A)^3 \ll 1 \tag{1.1}$$

is assumed small.

Let strain localization set in at time t in a thin layer Σ containing a certain number of pores, which is oriented in a certain fashion with respect to the principal directions X_i (Fig. 1). The velocity field within the layer is

$$u_i = g_i(X_i) \quad (i = 1, 2, 3). \tag{1.2}$$

The functions g_i should satisfy the conditions for velocity continuity at the boundaries of the layer:

$$g_i(X_i)|^+ = u_i^s|^+, \quad g_i(X_i)|^- = u_i^s|^-, \tag{1.3}$$

where the superscripts plus and minus relate to the internal and external boundaries, while the superscript s relates to the speed of the material outside the localization region. Superimposed rigid motion has no effect on the state of strain, so one can meet the symmetry condition at any point in the layer by choosing the transport velocity:

$$g_i(X_i)|^+ = -g_i(X_i)|^-. \tag{1.4}$$

We use (1.3) and (1.4) to write the boundary conditions for the g_i in a small region around this point as

$$g_i(X_i)|^+ = -g_i(X_i)|^- = \frac{1}{2}(u_i^s|^+ - u_i^s|^-) = \frac{1}{2}[u_i^s]. \tag{1.5}$$

It follows from (1.2) and (1.5) that the state of strain within the localization region is determined by the increment in the velocity vector $[u_i^s]$ at the boundaries.

We resolve the vector $[u_i^s]$ into the normal component [w] and the tangential one [v], both in relation to layer Σ, and introduce a local Cartesian coordinate system x, y, z, in which the z axis coincides with the normal $\bar{n}$ to the layer Σ and the y axis coincides with the direction of [v], while the origin coincides with the center of the arbitrary pore O (Fig. 1). For $\theta \ll 1$ we can neglect the interaction between pores, which enables us to restrict consideration to an element of the layer with mean dimensions 2A along the x and y axes in the local system (hatched in Fig. 1). According to (1.5), the state within this element is determined by the solution for the stretching (compression) with shear of a thin layer with rates ±[w]/2, ±[v]/2 correspondingly. As this shear should occur on the weakest section, the layer thickness should be comparable with the pore height 2h. Also, the incompressibility condition and symmetry considerations imply that the flow of material through the boundaries of the element x = ±A, y = ±A is zero, while that through the boundaries z = ±h is related to change in pore volume. To simplify the analysis, we replace the actual pore shape by an equilateral parallelepiped in such a way as to retain the mean porosity of (1.1) and the ratio of the dimensions along the axes of the local coordinate system. Figure 2a shows the final geometry of this element.

To construct the solution, we first consider stretching (compression) with shear for a thin rectangular band with stresses applied to the edges (Fig. 2b):

$$\sigma_x = q_x \text{ at } x = \pm L, \; \sigma_y = q_y \text{ at } y = \pm B. \tag{1.6}$$

The kinematic boundary conditions are defined by

$$m = [w]/[v]. \tag{1.7}$$

We assume that $m \ll 1$, i.e., the state in the layer approximates to simple shear, for which m = 0. For m = 0, there are maximal tangential stresses $\tau_{zy} = k$ at the constant surfaces z = ±h, where k is the yield point of the matrix material in shear. If $m \neq 0$, the inherent strain in the band changes the velocities of the flow relative to external volumes of the material, which is accompanied by redistribution of the frictional forces at the boundaries z = ±h. As m is small, we replace the actual tangential-stress distribution at the boundaries by the mean values:

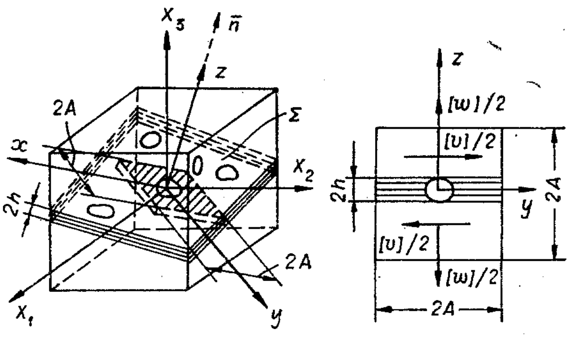

Fig. 1

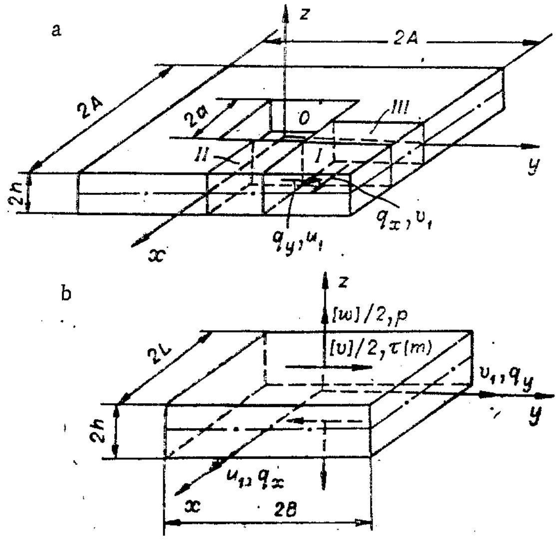

Fig. 2

$$\tau_{zx} \simeq 0, \quad \tau_{zy} \simeq \frac{1}{4LB} \int \tau_{zy} dx dy = \tau(m) \quad \text{at} \quad z = \pm h. \tag{1.8}$$

Here τ(m) is the desired function of m. Equations (1.6)–(1.8) define the boundary conditions.

For a sufficiently thin band $h \ll L$, $h \ll B$ and a small m, we can neglect the changes in the stress components over the thickness of the layer:

$$\partial \sigma_{ij} / \partial z \simeq 0. \tag{1.9}$$

We substitute (1.9) into the equilibrium equations

$$\partial \sigma_{ij} / \partial x_i = 0 \quad (i = 1,\ 2,\ 3,\ x_1 = x,\ x_2 = y,\ x_3 = z)$$

and integrate them together with (1.6) and (1.8) to get that the state of strain in the band corresponds to the homogeneous solution

$$\tau_{xz} = \tau_{xy} = 0,\ \tau_{zy} = \tau(m),\ \sigma_x = q_x,\ \sigma_y = q_y,\ \sigma_z = p, \tag{1.10}$$

where p is the normal pressure at the boundaries $z = \pm h$. The components of (1.10) should satisfy the Mises plasticity condition:

$$f \equiv (q_x - q_y)^2 + (q_y - p)^2 + (p - q_x)^2 + 6\tau^2(m) - 6k^2 = 0. \tag{1.11}$$

We now determine the state of strain in the band. According to the associated plastic-flow law, the components of the strain-rate tensor will be

$$\begin{gathered} \xi_x = \lambda \frac{\partial f}{\partial \sigma_x} = \frac{\lambda}{3}(2q_x - q_y - p), \quad \xi_y = \frac{\lambda}{3}(2q_y - q_x - p), \\ \xi_z = \frac{\lambda}{3}(2p - q_x - q_y), \quad \eta_{zy} = 2\lambda\tau(m), \quad \eta_{xy} = \eta_{zx} = 0 \quad (\lambda > 0). \end{gathered} \tag{1.12}$$

In the same way as (1.10), the solution to (1.12) corresponds to a homogeneous state of strain throughout the band. This enables us to express (1.12) in terms of the velocities at the edges:

$$\xi_x = u_1/L,\ \xi_y = v_1/B,\ \xi_z = [w]/2h,\ \eta_{zy} = [v]/2h, \tag{1.13}$$

where the quantities u_1 and v_1 relate to points in the middle section $z = 0$ (Fig. 2b). Substitution of (1.12) and (1.13) into (1.7) gives

$$m = \xi_z / \eta_{zy} = (2p - q_x - q_y)/6\tau(m), \tag{1.14}$$

or

$$\tau(m) = (2p - q_x - q_y)/6m. \tag{1.15}$$

If m is given, then (1.11) and (1.15) can be solved for the unknown quantities p and τ(m). On the other hand, if the normal pressure p at the contact is given, then m and τ(m) can be found from (1.11) and (1.14). Then all the state parameters can be determined.

In this case $m \ll 1$, the solution to (1.11) and (1.14) up to quantities of the second order of smallness takes the form

$$p \simeq (q_x + q_y)/2 + 3mk, \quad m \simeq (2p - q_x - q_y)/6k, \quad \tau(m) \simeq k. \tag{1.16}$$

The parameters of the state of strain are

$$\xi_x = ([v]/8kh)(q_x - q_y - 2mk), \quad \xi_y = ([v]/8kh)(q_y - q_x - 2mk),$$
$$\xi_z = [v]m/2h, \quad \eta_{zy} = [v]/2h, \tag{1.17}$$

and the speeds at the edges of the band are

$$u_1 = ([v]L/8kh)(q_x - q_y - 2mk), \quad v_1 = ([v]B/8kh)(q_y - q_x - 2mk). \tag{1.18}$$

2. We use this solution to examine the state in a layer element containing a pore (Fig. 2a). Because of the symmetry, we restrict consideration to a quarter of the element, which we divide up into three homogeneously deformed parts I, II, and III. The kinematic parameter of (1.7) remains constant for all these, while condition (1.1) implies that $m \ll 1$ (clearly, $m \to 0$ for $\theta \to 0$). At the boundaries $z = \pm h$, (1.8) is obeyed, while at the boundaries $x = a$ and $y = a$ the normal velocities and stresses are continuous (Fig. 2a shows the quantities relating to regions II and III), while at the boundaries $x = A$, $y = A$, $x = 0$, and $y = 0$ the normal velocities in the median section are zero. This means that the solution to (1.16)-(1.18) with the corresponding parameter choice applies for each of the regions.

From (1.18) we write the velocities at the boundaries:

$$u_1 = -\frac{[v](A-a)}{8kh}(q_x - q_y - 2mk) \quad \text{at} \quad x = a,$$
$$v_1 = -\frac{[v](A-a)}{8kh}(q_y - q_x - 2mk) \quad \text{at} \quad y = a \tag{2.1}$$

for region I;

$$u_1 = \frac{[v](A-a)}{8kh}(q_y + 2mk) \quad \text{at} \quad x = a,$$
$$v_1 = \frac{[v]a}{8kh}(q_y - 2mk) \quad \text{at} \quad y = a \tag{2.2}$$

for region II; and

$$u_1 = \frac{[v]a}{8kh}(q_x - 2mk) \quad \text{at} \quad x = a, \quad v_1 = \frac{[v](A-a)}{8kh}(q_x + 2mk) \quad \text{at} \quad y = a \tag{2.3}$$

for region III. We equate the corresponding equations (2.1)-(2.3) to find the unknown stresses at the boundaries between the regions;

$$q_x = q_y = q = 2mkA/a. \tag{2.4}$$

The normal pressure for each of the regions is

$$p_{\mathrm{I}} = mk(3 + 2A/a), \quad p_{\mathrm{II}} = p_{\mathrm{III}} = mk(3 + A/a).$$

Then the mean pressure on the shear area of the layer element is

$$p = p_{\mathrm{I}}\left(\frac{A-a}{A}\right)^2 + 2p_{\mathrm{II}}\frac{(A-a)a}{A^2} \simeq mk(1 + 2A/a). \tag{2.5}$$

The quantity of (2.5) corresponds to the macroscopic value of the hydrostatic component of the stress tensor σ in the shear plane and is usually given. Then from (2.5) we have

$$m = \sigma a/[k(2A + a)]. \tag{2.6}$$

As regards the other equations in (2.2) and (2.3), we see that the speeds at the surfaces of the pores in the directions of the x and y axes are equal, while the pore grows or condenses isotropically in the shear plane. From (2.4) and (2.6) we have the corresponding growth rates:

$$u = v = [v]\sigma(A^2 - a^2)/[4kh(2A + a)]. \tag{2.7}$$

We now determine the pore size change during finite strain. From (2.7) we have the pore-size increments as

$$dh = [v]\sigma a dt/[4k(2A + a)], \quad da = [v]\sigma(A^2 - a^2)dt/[4kh(2A + a)], \tag{2.8}$$

whence

$$dh/da = 2ah/(A^2 - a^2).$$

We integrate this equation with the initial condition $a_0 = h_0$, which is a consequence of the property isotropy of the material in the initial state, to get

$$h = a_0\left(A^2 - a_0^2\right)/(A^2 - a^2). \tag{2.9}$$

Equations (2.8) and (2.9) can be solved explicitly for a and h. In accordance with (1.1), we restrict ourselves to the stage of pore growth where a/A is fairly small. Then (2.9) implies $h \simeq a_0$, while the second equation in (2.8) gives

$$a = a_0 + \sigma A\Gamma/4k, \tag{2.10}$$

where $\Gamma = [v]t/2a_0$ is the relative shear in the localization layer over time t. Therefore, the pores evolve isotropically in the localization region only in the shear plane, while the pore height remains close to the initial value. For $\sigma > 0$ the pores grow in the same way as viscous cracks, and their transverse dimensions change in proportion to the product of the shear Γ and the relative hydrostatic pressure σ/k; for $\sigma < 0$ there is the analogous pore closure process. In both cases, the pore shape becomes substantially nonequilibrium, which means that the mean-porosity parameter of (1.1) cannot be used as a characteristic during the localization stage. The corresponding quantity must be referred to the localization volume. From (2.10) we have for the porosity in a shear band

$$\theta = \left(\theta_0^{1/3} + \sigma\Gamma/4k\right)^2, \tag{2.11}$$

where θ_0 is the initial porosity (at t = 0). This process should be accompanied by a certain modification in the constituent equations describing the plastic behavior in the localization region. Although this micromechanical model is too crude to reveal some detailed features of these equations such as nodal points at the loading surface, nevertheless (1.17) and (2.6) indicate an explicit dependence on the hydrostatic pressure [6].

3. An example of a stationary localization region is provided by the velocity-discontinuity lines in an incompressible rigid-plastic material. There is always some slight porosity in a real metal, but when there is extensive plastic strain one observes narrow shear bands with high velocity gradients at the boundaries of the corresponding regions, which are close to discontinuities. In many instances of forging, rolling, and wire drawing, the material separates along these boundaries and viscous cracks are formed. The linearized solution in terms of the parameter of (1.1) can be used for the localization layer if the porosity is small:

$$u_i = u_i^0 + \theta u_i', \quad \xi_{ij} = \xi_{ij}^0 + \theta\xi_{ij}', \quad \sigma_{ij} = \sigma_{ij}^0 + \theta\sigma_{ij}', \tag{3.1}$$

where the quantities with zero superscripts correspond to a rigid-plastic body and the primed quantities remain to be determined. From (1.7), (2.4), and (2.5) we have as follows for the macroscopic strain rates in the layer:

$$\xi_x \simeq \xi_y \simeq \eta_{yx} \simeq \eta_{zx} \simeq 0, \; \xi_z = \sigma a[v]/[2kh(2A + a)], \; \eta_{zy} = [v]/2h,$$

so the rate of change of volume is

$$\xi = \sigma a[v]/[2kh(2A + a)]. \tag{3.2}$$

We substitute (3.1) into (3.2) and neglect quantities of the second order of smallness to get

$$\xi \simeq a\sigma^0[v^0]/2kh(2A + a).$$

Then up to terms of order θ^2, the porosity change in a shear band can be determined from the corresponding solution on a velocity-discontinuity line for an incompressible rigid-plastic material. The approach is of value in that one can use well-developed techniques in the theory of plasticity [11] in examining viscous failure in the localization region. For simplicity we restrict ourselves to the case of a planar strain state. Let Σ be a line of

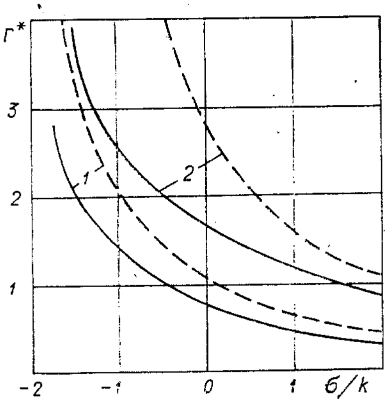

Fig. 3

velocity discontinuity in a rigid-plastic material, along which the following kinematic relations [11] apply:

$$w^0 = w^0|^+ = w^0|^-, \quad [v^0] = |v^0|^+ - v^0|^-|.$$

There is a finite shear on passage through this line:

$$\Gamma^0 = [v^0]/w^0. \tag{3.3}$$

We substitute (3.3) into (2.11) in accordance with the above to get the porosity θ after intersecting the lines Σ

$$\theta = \left(\theta_0^{1/3} + \frac{\sigma^0 [v^0]}{4kw^0}\right)^2. \tag{3.4}$$

On current concepts [1, 2], the viscous-failure mechanism in a plastic metal is determined by the sequentially occurring processes of pore nucleation, growth, and coalescence at different levels. The contributions from the nucleation and coalescence stages to the overall strain history are unimportant, and they can be neglected, and the viscous-failure criterion can be formulated from the condition for the attainment of a critical porosity θ* [12]. In macroscopic failure, this state must extend to some minimal representative volume ΔV containing a sufficiently large number N of pores and microstructure elements. As there are different pore-nucleation probabilities and growth conditions at the microstructure elements, (3.4) must be averaged over the ensemble of realizations N within the volume ΔV with allowance for the nonuniformity in the distributions of the microstresses and microstrains. If we introduce the structure parameters <σ'> and η [12] and neglect the nonuniformity of the macroscopic state within ΔV, then averaging of (3.4) at the instant when the critical porosity is attained gives the condition for macroscopic failure within the localization region:

$$\Gamma^* = [4k(\langle\theta^*\rangle^{1/2} - \langle\theta_0\rangle^{1/3})]/[\eta(\sigma^0 + \langle\sigma'\rangle)]. \tag{3.5}$$

Here <σ'> is the average value of the spherical component in the microstress tensor near the pores, η is the corresponding parameter characterizing the microstrain inhomogeneity, Γ* is the limiting shear-strain intensity in the localization region at failure, and the quantities in angular brackets relate to the mean values. One sees that the solution to (3.5) exists only for $\sigma^0 + \langle\sigma'\rangle > 0$, when pore growth occurs; for $\sigma^0 + \langle\sigma'\rangle < 0$, strain in the shear bands is accompanied by pore closure.

In order to use (3.5), one has to know the quantities <σ'>, η, <σ*> as characteristics of the material in the relevant state. These quantities have to be determined by experiment for macroscopic description, and also because of the complexity in deriving theoretical estimates. As they are assumed to be independent of the scheme for the state of strain, like the other mechanical constants, one can use plasticity diagrams obtained in simple loading to derive them [13]. Figure 3 gives results from corresponding calculations from (3.5) similar to those considered in [12] for steel 45 (curve 1) and aluminum alloy AMg2 (curve 2). Here we have assumed $\theta_0 = 0$, $\theta^* = 0.2$. The dashed curves in Fig. 3 relate to experiments for the case [13] where a homogeneous state was provided in the working volumes and the pore growth approximated isotropic. The curves of Fig. 3 show that pronounced pore growth anisotropy in the shear plane results in considerable reduction in the limiting plasticity in the localization region. This difference demonstrates the effects of the various pore growth mechanisms in a homogeneously deformable region and in a shear band; in calculations for the average deformations referred to a finite volume for the latter case, the discrepancies between the curves become even more important [10, 11].

These results enable one to estimate the failure probability in localization regions when the shape of a metal is changed plastically. As the shear-strain intensity Γ^0 on the velocity-discontinuity lines for a rigid-plastic material is usually of the order of one [11], it follows from Fig. 3 that hydrostatic tensile stresses (or low compressive ones) produce the limiting states on the discontinuity lines before that at the other points in the deformation focus. The corresponding types of viscous failure are usually observed in the plastic working of metals in the form of forging press, axial cracks, and exfoliation along the boundaries of the plastic region and the extensive-shear lines.

LITERATURE CITED

1. F. McClintock, "Plastic aspects of viscous failure," in: Failure [Russian translation], H. Libowicz (ed.), Mir, Moscow (1976).
2. F. McClintock, "A criterion for viscous failure due to pore growth," Prikl. Mat. Mekh., No. 4 (1968).
3. J. R. Rice and D. M. Tracey, "On the ductile enlargement of voids in triaxial stress fields," J. Mech. and Phys. Solids, 17, No. 3 (1969).
4. R. J. Green, "Theory of plasticity in porous bodies," in: Mechanics [Russian translation], No. 4 (1973).
5. A. Gerson, "The continuum theory of viscous failure due to pore nucleation and growth. Part 1," Theoretical Principles of Engineering Calculations [in Russian], No. 1 (1977).
6. J. R. Rice, "Plastic-strain localization," in: Theoretical and Applied Mechanics: Proceedings of the 14th IUTAM International Congress [Russian translation], Mir, Moscow (1979).
7. C. A. Berg, "Plastic dilation and void interaction," in: Inelastic Behavior of Solids, M. F. Kannien, W. F. Adler, A. R. Rosenfeld, and R. I. Jaffe (eds.), McGraw-Hill, New York (1969).
8. S. N. Bandyopadhyay and N. Singh, "Stability of void growth in an incompressible solid under uniaxial tension and shear," in: Engineering Fracture Mechanics, 11, No. 4 (1979).
9. J. Christoffersen, Microlocalization, Report Dan. Cent. Appl. Math. Mech., No. 180 (1980).
10. H. Yamamoto, "Conditions for shear localization in the ductile fracture of void-containing materials," Int. J. Fract. Mech., 14, No. 4 (1978).
11. R. Hill, Mathematical Theory of Plasticity, Oxford University Press (1950).
12. V. M. Segal, "A criterion for viscous failure in plastic shape change in metals," Zh. Prikl. Mekh. Tekh. Fiz., No. 1 (1981).
13. V. L. Kolmogorov, Stresses, Strains, and Failure [in Russian], Metallurgiya, Moscow (1970).